

Minireview:
Metal Preferences and Metallation

Andrew W Foster, Deenah Osman and Nigel J
Robinson
J. Biol. Chem. published online August 26, 2014

CELL BIOLOGY

MICROBIOLOGY

Access the most updated version of this article at doi: [10.1074/jbc.R114.588145](https://doi.org/10.1074/jbc.R114.588145)

Find articles, minireviews, Reflections and Classics on similar topics on the [JBC Affinity Sites](#).

Alerts:

- [When this article is cited](#)
- [When a correction for this article is posted](#)

[Click here](#) to choose from all of JBC's e-mail alerts

This article cites 0 references, 0 of which can be accessed free at
<http://www.jbc.org/content/early/2014/08/26/jbc.R114.588145.full.html#ref-list-1>

Metal preferences and metallation

Andrew W. Foster, Deenah Osman and Nigel J. Robinson¹

*Department of Chemistry and School of Biological and Biomedical Sciences,
Durham University, DH1 3LE, UK*

Running title: *Metal preferences and metallation*

¹To whom correspondence should be addressed: e-mail: nigel.robinson@durham.ac.uk

Key words: Metallochaperone, metal-sensors, metalloenzymes, Irving-Williams series, polydisperse buffer, associative-exchange.

Abstract

The metal-binding preferences of most metalloproteins do not match their metal-requirements. Thus, metallation of an estimated 30% of metalloenzymes is aided by metal-delivery systems, with ~25% acquiring pre-assembled metal-cofactors. The remaining ~70% are presumed to compete for metals from buffered metal-pools. Metallation is further aided by maintaining the relative concentrations of these pools as an inverse function of the stabilities of the respective metal complexes. For example, magnesium enzymes always prefer to bind zinc and these metals dominate the metalloenzymes without metal-delivery systems. Therefore, the buffered concentration of zinc is held at least a million-fold below magnesium inside most cells.

This narrative sets out, with examples, how cells assist metallation. Such assistance is vital because the physical and chemical properties of proteins tend to select essential divalent metal ions with a ranked order of preference which follows the Irving-Williams series (1):



Competitive metals must be kept out of binding sites for the weaker-binding ions. Cupric ions are at the top of the series although their order with respect to zinc can flip (2). In the reducing conditions of the cytoplasm, cuprous (Cu^+) rather than cupric (Cu^{2+}) ions are expected to predominate but these ions can also form tight complexes, especially with sites that contain sulphur-ligands (3). In the periplasm of bacterial cells ferric (Fe^{3+}) rather than ferrous (Fe^{2+}) ions often dominate (4). Ferric ions are retained in solution in organic-

complexes which can be exceptionally tight and include binding proteins such as Fbp in the bacterial periplasm (5).

Because proteins are not rigid, the scope for steric-selection of metal-cofactors is imperfect. Mis-metallation can exploit a sub-set of ligands and/or distort the native binding geometry. Typically a protein becomes inactive if one or more residues of an active metal site are recruited to an alternative site, perhaps with alternative geometry, by a more competitive metal. For example, glyoxylase of *Clostridium acetobutylicum* (GlxI) is activated by nickel or cobalt, both of which assume octahedral geometries, while zinc binds tightly in trigonal bipyramidal geometry and inactivates this isoform of the enzyme (6).

Correct metallation *in vivo* is favoured because the cytoplasm is a metal-controlled environment. For example, two periplasmic cupins (manganese MncA and cupric CucA) from a model cyanobacterium bind metal via analogous ligand sets within analogous folds (Figure 1), yet *in vivo* they acquire different metals. MncA and CucA both show *in vitro* metal preferences which match the Irving-Williams series which is especially problematic for MncA. A 10,000 and a 100,000 -times excess of manganese is required at MncA-folding in order for manganese to outcompete cupric or zinc ions, respectively (7). Cuprous ions can also outcompete manganese. Manganese MncA has oxalate decarboxylase activity while neither the zinc nor the copper forms are active (7). CucA is a Sec-substrate which folds in the periplasm on secretion while MncA is a Tat-substrate. The Tat-system translocates pre-folded proteins and hence MncA folds within the cytoplasm before export (7,8). In this way, MncA entraps manganese before exposure to copper and zinc in the periplasm. In the cytoplasm, at the site of MncA folding, copper and zinc must be at least 10,000 and 100,000 -times less

available than manganese. This must reflect the relative buffered concentrations of these three metals plus, hypothetically, a manganese delivery system for MncA.

When metals compete with other metals for proteins

Metal-availability within cells is restricted such that proteins compete with other molecules, including other proteins, for limited pools of the most competitive metals. Dudev and Lim have assessed the physical and chemical properties of metals and proteins which influence metal preferences (9). These include valence, ionic radius, coordination-geometry, ligand number, second-shell ligands, effects of the protein matrix and ligand characteristics (net charge, dipole moment and polarisability, charge-donating/-accepting ability and denticity) (9). Despite these opportunities to tune metal preferences, *in vitro* metallation is typically aberrant when essential metals simply compete with each other for proteins (7).

Zinc and magnesium are the most commonly utilised metal-cofactors (~16 and ~9 % of all enzymes, respectively) (10), and dominate the subset of metalloenzymes lacking a defined delivery system, representing ~ 78 % of this group (Table 1). Empirically, zinc is known to replace magnesium to inactivate enzymes including β -galactosidase (11), tyrosine kinases (12), and magnesium alkaline phosphatase (13,14). The calculated free energies for replacing magnesium with zinc in rigid or flexible sites implies that zinc will always be favoured over magnesium in mono- and bi-nuclear binding pockets, with ΔG for replacement in flexible, neutral sites ranging from -10 to -29 kcal mol⁻¹ (15). The incorporation of magnesium into chlorophyll to metallate chlorophyll binding proteins is a special case which exploits delivery systems and is therefore considered separately in a later section of this minireview.

Iron and manganese are the next most common cofactors estimated to be exploited by ~ 8 % and ~ 6 % of enzymes (10). These ions account for most (~18 %) of the remaining fraction of metalloenzymes that are devoid of delivery systems, noting that another sub-set of iron enzymes do have metal-delivery systems and iron is commonly found in pre-assembled cofactors. The divalent ions of manganese and iron have similar ligand affinities, radii, coordination preferences and solvation free energies creating a distinct challenge for proteins to discern between these elements when they compete for a site (9).

Uncertain metallation *in vivo* and cambialistic proteins

With a few pioneering exceptions (16,17), the extent of mis-metallation *in vivo* is unknown. Current methods for native metallo-proteomics are neither global nor high throughput (7,18), and so the extent of post-translational regulation through metallation is unclear. The picture is further complicated because multiple metals support catalysis in so-called cambialistic enzymes. Acireductone dioxygenase (ARD) from *Klebsiella oxytoca* is currently a rare example of an enzyme which can catalyse two different reactions dependent upon metal occupancy (19). Iron-ARD is widespread and the nickel-ARD-dependent pathway has been observed in *Bacillus subtilis* and *Escherichia coli* but both forms have been recovered from *K. oxytoca*. However, there is currently no evidence that both forms of the enzyme confer a selective advantage to *K. oxytoca*. Fractional occupancies of ARD with nickel and iron remain to be investigated *in vivo*, as does the tantalising possibility that metallation is switched to match metabolic need.

Conformationally trapped metals and opportunities for proof-reading of metallation

There is scope for mis-metallated proteins to be selectively degraded, re-cycled or to remain in a partially unfolded state. A sub-set of metal-cofactors become kinetically trapped in proteins. The correct geometry can stabilise the fold, offering, in effect, the potential for proof-reading of metal-occupancy based upon second coordination shell interactions. For example, manganese in the copper-cupin CucA is readily replaced upon incubation with copper, but in the structurally related manganese-cupin MncA, manganese becomes trapped at folding and refractory to subsequent replacement by copper (7). Thus, folding and metal-trapping is uncoupled from manganese binding to CucA, where this is mis-metallation, but coupled to manganese binding in MncA. To date, *in vitro* biochemical studies of metal-binding preferences of proteins have not included protein folding chaperones such as Hsp70 or its co-chaperones and nucleotide exchange factors. Association of chaperones with exposed hydrophobic patches of nascent proteins impacts upon the energetics of protein folding (20), but it remains to be tested whether or not this sometimes imposes a bias in favour of the correct metal.

Metal delivery pathways

Fidelity in metallation with two competitive metals, nickel and copper, is typically assisted by metallochaperones (21-23). The term 'metallochaperone' describes a collection of proteins, for a diversity of metals, which differ in their biochemical mechanisms. Known nickel chaperones, which include HypB, interact with a battery of other proteins with consumption of nucleotide cofactors aiding metal insertion (21,22). When *Helicobacter pylori* HypB aberrantly binds zinc its GTPase activity is not triggered and in this way cofactor delivery becomes selective for nickel (24). Known copper chaperones do not require nucleotide cofactors. Both copper and nickel chaperones introduce a kinetic bias into the partitioning of metals by engaging in specific protein-protein interactions which recognise the correct partners (23). Such interactions also orientate the donor and acceptor ligands to encourage facile ligand-exchange (25).

Pre-assembled complex metal-cofactors include cobalamin (cobalt), iron-sulphur clusters, heme and siroheme (iron), molybdopterin (molybdenum), F430 (nickel) and chlorophyll (magnesium). Discrimination between these more elaborate molecular assemblies as opposed to individual metal ions at cofactor selection is less challenging, but nonetheless may be aided by delivery proteins: For example, monothiol glutaredoxins (Grx's) and BolA proteins play roles in [FeS] cluster delivery as well as iron sensing (26), with yeast strains deficient in Grx3 and 4 exhibiting defects in multiple iron-dependent enzymes (27,28); NarJ assists in the insertion of molybdopterin into nitrate reductase in *E. coli* cells (29), and CcmE functions as a heme chaperone in the periplasm of *E. coli*, delivering its cargo to CcmF for insertion into cytochrome *c* (30).

Metallochaperones that contribute towards fidelity in partitioning metals during complex cofactor assembly include chelatasers for heme, cobalamin and chlorophyll (31,32), and MoeA for molybdopterin (33). Ferrochelatasers, for example, can catalyse the insertion of metals other than iron into tetrapyrroles, such that zinc protoporphyrin IX becomes diagnostic for some iron deficiencies (34). The metal preferences and metallation of metallochaperones warrants investigation.

The majority of copper proteins are secreted and copper efflux from the cytosol is driven by P₁-type ATPases which acquire copper from metallochaperones such as Atx1 (35,36). Exactly how copper is then handed to nascent proteins post-secretion is the topic of current investigations.

Oddly, CucA in the cyanobacterial periplasm has impaired metallation in mutants missing copper-transporting P₁-type ATPases (CtaA and PacS) and the mutant periplasm is devoid of CucA but enriched with low M_r copper-complexes (37). Thus, copper is routed via the cytoplasm and the cyanobacterial copper chaperone Atx1, before export via a P₁-type ATPase in order to load CucA. Moreover, secretion of CucA seems to be coupled to copper efflux (37). A sub-set of P₁-type ATPases that have tight K_m and low V_{max}, do not confer copper-resistance but appear to support metal delivery to nascent cupro-proteins (38). There is evidence of interaction between *E. coli* periplasmic copper chaperone CusF and P₁-type ATPase CopA, while periplasmic copper chaperone CueP is required for metallation of SodCII in *Salmonella enterica* sv. Typhimurium (39,40).

Evaluating the contribution of delivery pathways to metallation

To estimate the fractions of metalloproteins that bind pre-assembled cofactors or are otherwise metallated via metallochaperones, the Metal-MACiE database has been interrogated. Metal-MACiE is a manually curated catalogue of enzymes which require metals for their catalytic mechanisms and for which a protein structure has been determined (41). Metal ions solely performing structural roles in proteins which are not enzymes are not annotated in Metal MACiE. This is liable to lead to an under-representation of zinc which is widely used in zinc fingers (42). With such limitations in mind, Metal MACiE can be used to make first approximations of the proportions of enzymes with various metal-centres. Table 1 lists the types of sites in the database, noting where proteins are known to assist in metal delivery directly to the enzyme (exemplified by nickel and copper), to a sub-cellular compartment containing the enzyme (exemplified by copper in the secretory system or periplasm), or to pre-formed metal-cofactors. In total, 30 % of metalloenzymes within the database are estimated to lie at the end of such delivery pathways, and metalloenzymes are estimated to account for almost half of all enzymes (43).

It is uncertain where most metallochaperones acquire metal and to what extent their relative metal-affinities correspond to the metal-requirements of the delivery pathways. Cyanobacteria are useful models for exploring partitioning among metallochaperones. In common with other photosynthetic organisms they have a

high demand for metals (44), but also they have delivery proteins for an especially wide range of metals: Atx1 for copper to thylakoids (45), UreE and HypA/B for nickel to urease and hydrogenase (46), ferrochelatase for iron to heme and siroheme (47), magnesium chelatase for magnesium to chlorophyll (48), CbiX for cobalt to cobalamin (plants in contrast do not make cobalamin) (49), MoeA for molybdenum to molybdopterin, CyaY for iron to iron sulphur clusters and possibly PrtA for manganese to photosystem II (50). A set of metal-competition experiments between the purified cyanobacterial metallochaperones could establish whether or not their relative metal-affinities simply enable metals to partition to the correct delivery pathway. This in turn would resolve the metallation-challenge for ~ 30 % of metalloenzymes.

Alternatively, metallochaperones might directly acquire metal from importers assisted by specific protein interactions. The idea that inward metal transport is coupled to the loading of delivery pathways, to channel metals to sites of metalloenzyme assembly, is widely envisioned but sparsely evidenced. Notably, analyses of yeast mutants did not identify any single copper donor for either of two copper metallochaperones (51). Nonetheless, there is evidence that the copper chaperone for superoxide dismutase (CCS) can interact with membranes and with the copper importer Ctr1 (52), and metal transfer to Atx1 has also been observed *in vitro* using a cytosolic domain of Ctr1 (53). Nickel imported by the Nik-system is destined for hydrogenase and largely unavailable to nickel-responsive transcriptional regulators (54), which might also suggest direct hand-over of nickel to HypA/B. However, evidence that the substrate for the Nik-importer is a nickel-histidine complex provides an alternative explanation for these observations if HypA/B can preferentially acquire nickel from nickel-histidine (55). There is evidence that a mitochondrial iron importer mitoferrin-1 interacts with a ferrochelatase for heme biogenesis (56). This iron supply pathway cannot be 'hard-wired' exclusively for iron if zinc protoporphyrin IX accumulates under iron deficiency (34). Iron sulphur clusters are the targets for surplus cobalt and copper (57-60). Both cobalt and copper directly destabilise the assembled cluster on the scaffold proteins and, at least for cobalt, it is known that the resultant mixed cluster can be delivered to apo-proteins (58,59). Thus, imperfect metal preferences of delivery systems can sometimes propagate mis-metallation.

Metallochaperone catalysed delivery of the more competitive metals, such as nickel and copper,

enables cells to more efficiently cofactor a sub-set of proteins with these ions. But viewed from a different perspective, such metal delivery supports metallation at low buffered concentrations sufficient to exclude these elements from binding sites for metals lower down the Irving-Williams series (1). For example, cyanobacterial mutants missing the copper metallochaperone Atx1 show phenotypes indicative of the mis-metallation of binding sites for other metals with copper (61).

The set points for metal homeostasis

The buffered (rather than total) set points for metals can vary between cell types, intracellular compartments and throughout the lifetime of a cell. Nonetheless, magnesium appears to be universally held at ~ 10^{-3} M inside cells (Figure 2, grey bar), about ten times less than the concentration in sea water and ten times more than typical concentrations in fresh water (62,63). Proteins that require ferrous ions often exhibit affinities of ~ 10^{-7} M which is suggested to match the ferrous concentration in the sulphide rich anaerobic conditions when life first evolved (64). By determining the ferrous-affinity of glutathione (glutathione has a concentration of ~ 2 to 10 mM within the cytoplasm), and assuming that this complex is a major component of the cytosolic iron pool, a value in the region of 10^{-6} to 10^{-7} M for the buffered concentration of ferrous iron is plausible (65) (Figure 2, grey bar).

The cytosolic concentration of manganese has been estimated to be comparable to ferrous iron (66,67) (Figure 2, grey bar). However, manganese concentrations may be elevated within organelles such as the chloroplast or mitochondria where there is high demand. In a bacterial cytosol the concentration of manganese can vary. For example, in response to oxidants, manganese is elevated to correctly metallate manganese SOD (16). Nickel- and cobalt-requiring enzymes are thought to have been more prevalent in early anaerobic life and Fraústo da Silva and Williams suggest that these two metals are unlikely to have ever exceeded 10^{-10} M in the cytosol (62) (Figure 2, grey bars).

Zinc binding sites in most proteins have affinities which are typically 10^{-11} M or tighter (68). The use of either synthetic or genetically encoded zinc-responsive fluorophores has placed buffered zinc concentrations within the cytosol of bacteria and eukaryotic cells in the 10^{-12} to 10^{-10} M range (69-72). Buffered cytosolic copper concentrations have been estimated to be ~ 10^{-15} M or less using copper responsive fluorophores (73,74) (Figure 2,

grey bar). In yeast, copper zinc superoxide dismutase (SOD1) has a copper affinity of 10^{-15} M but requires the CCS metallochaperone for activation *in vivo*. Consequently, it was inferred that copper must be buffered below 10^{-15} M (75). CCS additionally catalyses the formation of a vital disulphide bond within SOD1 (76), providing an alternative explanation for inactivity of SOD1 in CCS deficient cells.

What sustains these different buffered metal concentrations? An expectation is that this relates to detection thresholds of sensors that control homeostasis for the respective metals. There are pitfalls in the estimation of K_{Metal} , especially for tighter binding elements (77), generating a litter of erroneous values. Nonetheless, mindful of this caveat, a remarkable correlation exists between estimates of K_{Metal} for metal-sensors and estimates for buffered cytosolic metal concentrations (Figure 2). This observation is consistent with the intracellular set point for metal homeostasis being a function of these sensor-affinities. By setting the metal-affinities of metal-sensors such that those for the most competitive metals are the tightest, the control of metal-efflux, metal-influx, metal-sequestration and the switching of metabolism to spare limiting metals, is thus primed to maintain the buffered metal concentrations as an inverse function of the Irving Williams series. Under this regime, subtle differences in the relative metal preferences of metalloenzymes now become sufficient to enable correct *in vivo* metallation.

How a cells' set of metal-sensors act in concert to discern metals one-from-another

The actions of metal-sensors help maintain buffered metal concentrations, and these concentrations in turn influence which metals are acquired by $\sim 70\%$ of metalloenzymes. Thus metal-specificity of metal-sensors becomes a dominant factor in the fidelity of metallation. The proportion also becomes even higher than 70% if some metallochaperones are metallated from buffered metal-pools. Metal-sensing, DNA-binding, transcriptional regulators have been extensively characterised in bacteria (78,79), and identified for copper, iron, and zinc in yeast (80,81). However, where metal-affinities have been measured for multiple metals, the metal preferences of bacterial metal-sensor proteins again tend to simply abide by the Irving-Williams series (78,79,82).

Affinity, access (kinetics) and allostery: A series of publications in the first decade of this century,

revealed that metal-specificity of metal-sensors can be determined by three factors. First, metal-affinity contributes towards metal-selectivity. Second, the allosteric mechanism connecting metal-binding to altered DNA-binding or to gene-activation, can respond selectively to different metals. Finally, the kinetics of access can differ for different sensors, for example due to delivery proteins (10,82).

Relative-affinity, -access and -allostery: Since 2010 it has become evident that affinity, allostery and access operate as relative parameters in a set of sensors (83-85). Such observations are now possible because sufficiently large numbers of bacterial metal-sensors have been characterised. Metal-selectivity is now seen to result from the concerted actions of a cells complement of metal-sensors. In this manner specificity is not constrained by absolute metal preferences (10,82). The best-sensor in the set is the sensor that responds. But what defines the best in the set for each metal?

Recent studies of the metal-sensors of the model organism *Synechocystis* PCC 6803 exemplify the contributions of relative-affinity, relative-allostery and relative-access. By examining one sensor from each family of metal-sensors present in this organism, the parameter correlating with selective metal detection was found to vary from metal-to-metal (Figure 3). Importantly, the absolute metal preferences as reflected in K_{Metal} values of InrS (nickel responsive efflux de-repressor), CoaR (cobalt responsive efflux activator), ZiaR and Zur (zinc responsive efflux de-repressor and influx co-repressor, respectively) (61,83,86,87), do not universally match their metal specificities *in vivo*. Rather, the detection of nickel correlates with relative nickel affinity, the detection of zinc correlates with relative free energy coupling DNA-binding to zinc-binding (relative allostery), but a substantial kinetic contribution is invoked in the selective detection of cobalt (relative access) (83-85) (Figure 3).

To elaborate, InrS possesses the tightest nickel affinity in this set of metal-sensors (83). Thus, as the buffered concentration of nickel rises, provided the distribution of nickel among the sensors approximates to the thermodynamic equilibrium state, InrS will trigger nickel efflux before the concentration becomes sufficiently high for nickel to aberrantly bind to any of the other sensors (Figure 3a) (83). This assumes roughly equivalent numbers of molecules of each sensor per cell (a parameter which in future needs to be measured). Cognisant of the challenges in determining protein-metal affinities and noting the

weak $K_{Ni(II)}$ of ZiaR and Zur, a series of inter-protein competition experiments also confirmed that nickel partitions from each of the other sensors to InrS (83).

In contrast to nickel, cobalt affinities do not correlate with *in vivo* specificities, rather, cobalt sensing CoaR has the weakest $K_{Co(II)}$ of the set of sensors (84), (Figure 3a). Moreover *in vitro*, cobalt promotes DNA-association by Zur and DNA-dissociation by ZiaR, yet neither ZiaR nor Zur respond to cobalt *in vivo* under conditions when CoaR responds (84). This implies that cobalt is channelled to CoaR and away from ZiaR and Zur with their tighter cobalt affinities. There is evidence that CoaR is membrane-associated and cobalt acquisition may involve channelling via the cobalamin biosynthetic complex which is also membrane-associated. Additionally, there is evidence that CoaR may not solely sense cobalt directly, but also detect an intermediate in the B₁₂ assembly pathway (84). In summary, CoaR has preferential access to the cobalt effector relative to ZiaR and Zur.

The zinc affinity of InrS is comparable to the sensory sites of ZiaR and Zur (Figure 3a), yet following prolonged zinc exposure, ZiaR responds but InrS does not. Critically, although the allosteric mechanism of InrS is capable of responding to zinc, the coupling free energy linking zinc-binding to DNA-binding ($\Delta G_C^{zinc \cdot sensor \cdot DNA}$) is greater for ZiaR than for InrS (85), (Figure 3b). In short, zinc is a more effective de-repressor of ZiaR than of InrS. Thus, at some equivalent fractional zinc occupancies a greater proportion of InrS relative to ZiaR will be bound to DNA. InrS can thereby repress its gene target while the ZiaR target remains de-repressed. This exemplifies how relative coupling free energy ΔG_C , that is relative allosteric effectiveness, in a complement of metal-sensors can also dictate selectivity (Figure 3b).

Improbable kinetics and associative metallation

Metal affinities of metal-sensors for the most competitive metals such as nickel, zinc and copper are so tight that it is not credible for metal partitioning to and from solution to reach equilibrium in a viable timeframe. The off-rates are too slow. But this assumes dissociative metal-exchange. As an alternative, associative metal-exchange can occur to/from labile metal sites of proteins (including metal-sensors) and components of a polydisperse buffer. This ill-defined buffer is composed of small molecules such as amino acids, glutathione, organic acids and inorganic-ligands,

plus weak adventitious ligands on the surface of macromolecules, specific buffering proteins and a sub-set of the delivery proteins. Rates of metal exchange in cells can thus be unexpectedly fast, and swiftly approach the equilibrium state. Moreover, such a process of associative ligand-exchange through a polydisperse buffer can operate at buffered concentrations below 10^{-9} M, the theoretical threshold for one atom per cell volume in a bacterium such as *E. coli* (88).

For the most competitive metals the fully hydrated pool is indeed estimated to be below 10^{-9} M and thus equates to less than one (free) atom per cell at any instant (88,89) (Figure 2). In relation to Figure 3 and the example in the preceding section, InrS does transiently respond to zinc *in vivo* while the response of ZiaR is persistent. The buffered concentration of zinc would have to fall below 10^{-11} M for a protein with the $K_{Zn(II)}$ of InrS to have less than full zinc-occupancy in order to restore repression. Under these conditions, persistent ZiaR must therefore detect a pool of exchangeable zinc which is buffered at least two orders of magnitude below $\sim 10^{-9}$ M (85). One explanation is that ZiaR is metallated through associative ligand exchange with a polydisperse buffer rather than depending upon a hydrated pool of zinc ions. By way of illustration, the equations in Figure 4 represent the transfer of zinc from InrS to ZiaR (i) by a dissociative process requiring the slow release of zinc from InrS to the hydrated state, and (ii) by potentially swift associative exchange with ligands of a buffer.

Prospective: The elements of biotechnology and biomedicine

With such a large proportion of enzymes requiring metals, discord between their metal-binding preferences and metal-requirements has implications for biological chemistry, and applications in biomedicine and biotechnology. For example, knowledge of the *in vivo* metallation states of components of metabolic- and signalling-networks is required to improve the accuracy of systems biology computations. Synthetic biology aims to engineer cells for new purposes. Success may often depend upon an ability to coincidentally re-wire the circuitry for enzyme metallation.

Acknowledgements

Work in the authors' lab is supported by BBSRC research grants BB/K00817X/1 and BB/J017787/1.

References

1. Irving, H., and Williams, R. J. (1948) Order of stability of metal complexes. *Nature* **162**, 746-747
2. Johnson, D. A., and Nelson, P. G. (1995) Factors determining the ligand field stabilization energies of the hexaaqua 2+ complexes of the first transition series and the Irving-Williams order. *Inorg. Chem.* **34**, 5666-5671
3. Davis, A. V., and O'Halloran, T. V. (2008) A place for thioether chemistry in cellular copper ion recognition and trafficking. *Nat. Chem. Biol.* **4**, 148-151
4. Schalk, I. J., Yue, W. W., and Buchanan, S. K. (2004) Recognition of iron-free siderophores by TonB-dependent iron transporters. *Mol. Microbiol.* **54**, 14-22
5. Parker Siburt, C. J., Mietzner, T. A., and Crumbliss, A. L. (2012) FbpA--a bacterial transferrin with more to offer. *Biochim. Biophys. Acta* **1820**, 379-392
6. Suttisansanee, U., Lau, K., Lagishetty, S., Rao, K. N., Swaminathan, S., Sauder, J. M., Burley, S. K., and Honek, J. F. (2011) Structural variation in bacterial glyoxalase I enzymes: investigation of the metalloenzyme glyoxalase I from *Clostridium acetobutylicum*. *J. Biol. Chem.* **286**, 38367-38374
7. Tottey, S., Waldron, K. J., Firbank, S. J., Reale, B., Bessant, C., Sato, K., Cheek, T. R., Gray, J., Banfield, M. J., Dennison, C., and Robinson, N. J. (2008) Protein-folding location can regulate manganese-binding versus copper- or zinc-binding. *Nature* **455**, 1138-1142
8. Kudva, R., Denks, K., Kuhn, P., Vogt, A., Muller, M., and Koch, H. G. (2013) Protein translocation across the inner membrane of Gram-negative bacteria: the Sec and Tat dependent protein transport pathways. *Res. Microbiol.* **164**, 505-534
9. Dudev, T., and Lim, C. (2014) Competition among metal ions for protein binding sites: determinants of metal ion selectivity in proteins. *Chem. Rev.* **114**, 538-556
10. Waldron, K. J., Rutherford, J. C., Ford, D., and Robinson, N. J. (2009) Metalloproteins and metal sensing. *Nature* **460**, 823-830
11. Fernandes, S., Geueke, B., Delgado, O., Coleman, J., and Hatti-Kaul, R. (2002) Beta-galactosidase from a cold-adapted bacterium: purification, characterization and application for lactose hydrolysis. *Appl. Microbiol. Biotechnol.* **58**, 313-321
12. Sun, G., and Budde, R. J. (1999) Substitution studies of the second divalent metal cation requirement of protein tyrosine kinase CSK. *Biochemistry* **38**, 5659-5665
13. Ciancaglini, P., Pizauro, J. M., Curti, C., Tedesco, A. C., and Leone, F. A. (1990) Effect of membrane moiety and magnesium ions on the inhibition of matrix-induced alkaline phosphatase by zinc ions. *Int. J. Biochem.* **22**, 747-751
14. Hung, H. C., and Chang, G. G. (2001) Differentiation of the slow-binding mechanism for magnesium ion activation and zinc ion inhibition of human placental alkaline phosphatase. *Protein Sci.* **10**, 34-45
15. Yang, T. Y., Dudev, T., and Lim, C. (2008) Mononuclear versus binuclear metal-binding sites: metal-binding affinity and selectivity from PDB survey and DFT/CDM calculations. *J. Am. Chem. Soc.* **130**, 3844-3852
16. Imlay, J. A. (2014) This set. *J. Biol. Chem.*
17. Stubbe, J. (2014) This set. *J. Biol. Chem.*
18. Cvetkovic, A., Menon, A. L., Thorgersen, M. P., Scott, J. W., Poole, F. L., 2nd, Jenney, F. E., Jr., Lancaster, W. A., Praisman, J. L., Shanmukh, S., Vaccaro, B. J., Trauger, S. A., Kalisiak, E., Apon, J. V., Siuzdak, G., Yannone, S. M., Tainer, J. A., and Adams, M. W. (2010) Microbial metalloproteomes are largely uncharacterized. *Nature* **466**, 779-782

19. Dai, Y., Wensink, P. C., and Abeles, R. H. (1999) One protein, two enzymes. *J. Biol. Chem.* **274**, 1193-1195
20. Hartl, F. U., and Hayer-Hartl, M. (2002) Molecular chaperones in the cytosol: from nascent chain to folded protein. *Science* **295**, 1852-1858
21. Higgins, K. A., Carr, C. E., and Maroney, M. J. (2012) Specific metal recognition in nickel trafficking. *Biochemistry* **51**, 7816-7832
22. Kaluarachchi, H., Chan Chung, K. C., and Zamble, D. B. (2010) Microbial nickel proteins. *Nat. Prod. Rep.* **27**, 681-694
23. Robinson, N. J., and Winge, D. R. (2010) Copper metallochaperones. *Annu. Rev. Biochem.* **79**, 537-562
24. Sydor, A. M., Lebrette, H., Ariyakumaran, R., Cavazza, C., and Zamble, D. B. (2014) Relationship between Ni(II) and Zn(II) coordination and nucleotide binding by the *Helicobacter pylori* [NiFe]-hydrogenase and urease maturation factor HypB. *J. Biol. Chem.* **289**, 3828-3841
25. Banci, L., Bertini, I., Cantini, F., Felli, I. C., Gonnelli, L., Hadjiladis, N., Pierattelli, R., Rosato, A., and Voulgaris, P. (2006) The Atx1-Ccc2 complex is a metal-mediated protein-protein interaction. *Nat. Chem. Biol.* **2**, 367-368
26. Mapolelo, D. T., Zhang, B., Randeniya, S., Albetel, A. N., Li, H., Couturier, J., Outten, C. E., Rouhier, N., and Johnson, M. K. (2013) Monothiol glutaredoxins and A-type proteins: partners in Fe-S cluster trafficking. *Dalton Trans.* **42**, 3107-3115
27. Ojeda, L., Keller, G., Muhlenhoff, U., Rutherford, J. C., Lill, R., and Winge, D. R. (2006) Role of glutaredoxin-3 and glutaredoxin-4 in the iron regulation of the Aft1 transcriptional activator in *Saccharomyces cerevisiae*. *J. Biol. Chem.* **281**, 17661-17669
28. Muhlenhoff, U., Molik, S., Godoy, J. R., Uzarska, M. A., Richter, N., Seubert, A., Zhang, Y., Stubbe, J., Pierrel, F., Herrero, E., Lillig, C. H., and Lill, R. (2010) Cytosolic monothiol glutaredoxins function in intracellular iron sensing and trafficking via their bound iron-sulfur cluster. *Cell Metab.* **12**, 373-385
29. Vergnes, A., Pommier, J., Toci, R., Blasco, F., Giordano, G., and Magalon, A. (2006) NarJ chaperone binds on two distinct sites of the aponitrate reductase of *Escherichia coli* to coordinate molybdenum cofactor insertion and assembly. *J. Biol. Chem.* **281**, 2170-2176
30. San Francisco, B., and Kranz, R. G. (2014) Interaction of holoCcmE with CcmF in heme trafficking and cytochrome *c* biosynthesis. *J. Mol. Biol.* **426**, 570-585
31. Schubert, H. L., Raux, E., Wilson, K. S., and Warren, M. J. (1999) Common chelatase design in the branched tetrapyrrole pathways of heme and anaerobic cobalamin synthesis. *Biochemistry* **38**, 10660-10669
32. Tanaka, R., and Tanaka, A. (2007) Tetrapyrrole biosynthesis in higher plants. *Annu. Rev. Plant Biol.* **58**, 321-346
33. Sandu, C., and Brandsch, R. (2002) Evidence for MoeA-dependent formation of the molybdenum cofactor from molybdate and molybdopterin in *Escherichia coli*. *Arch. Microbiol.* **178**, 465-470
34. Labbe, R. F., Vreman, H. J., and Stevenson, D. K. (1999) Zinc protoporphyrin: A metabolite with a mission. *Clin. Chem.* **45**, 2060-2072
35. Larin, D., Mekios, C., Das, K., Ross, B., Yang, A. S., and Gilliam, T. C. (1999) Characterization of the interaction between the Wilson and Menkes disease proteins and the cytoplasmic copper chaperone, HAH1p. *J. Biol. Chem.* **274**, 28497-28504
36. Lin, S. J., Pufahl, R. A., Dancis, A., O'Halloran, T. V., and Culotta, V. C. (1997) A role for the *Saccharomyces cerevisiae* ATX1 gene in copper trafficking and iron transport. *J. Biol. Chem.* **272**, 9215-9220
37. Waldron, K. J., Firbank, S. J., Dainty, S. J., Perez-Rama, M., Tottey, S., and Robinson, N. J. (2010) Structure and metal loading of a soluble periplasm cuproprotein. *J. Biol. Chem.* **285**, 32504-32511
38. Raimunda, D., Gonzalez-Guerrero, M., Leeber, B. W., 3rd, and Arguello, J. M. (2011) The transport mechanism of bacterial Cu⁺-ATPases: distinct efflux rates adapted to different function. *BioMetals* **24**, 467-475

39. Padilla-Benavides, T., George Thompson, A. M., McEvoy, M. M., and Arguello, J. M. (2014) Mechanism of ATPase-mediated Cu⁺ Export and Delivery to Periplasmic Chaperones: The interaction of *Escherichia coli* CopA and CusF. *J. Biol. Chem.* **289**, 20492-20501
40. Osman, D., Patterson, C. J., Bailey, K., Fisher, K., Robinson, N. J., Rigby, S. E., and Cavet, J. S. (2013) The copper supply pathway to a *Salmonella* Cu,Zn-superoxide dismutase (SodCII) involves P(1B)-type ATPase copper efflux and periplasmic CueP. *Mol. Microbiol.* **87**, 466-477
41. Andreini, C., Bertini, I., Cavallaro, G., Holliday, G. L., and Thornton, J. M. (2009) Metal-MACiE: a database of metals involved in biological catalysis. *Bioinformatics* **25**, 2088-2089
42. Klug, A. (2010) The discovery of zinc fingers and their applications in gene regulation and genome manipulation. *Annu. Rev. Biochem.* **79**, 213-231
43. Andreini, C., Bertini, I., Cavallaro, G., Holliday, G. L., and Thornton, J. M. (2008) Metal ions in biological catalysis: from enzyme databases to general principles. *J. Biol. Inorg. Chem.* **13**, 1205-1218
44. Merchant, S. S. (2014) This set. *J. Biol. Chem*
45. Tottey, S., Rondet, S. A., Borrelly, G. P., Robinson, P. J., Rich, P. R., and Robinson, N. J. (2002) A copper metallochaperone for photosynthesis and respiration reveals metal-specific targets, interaction with an importer, and alternative sites for copper acquisition. *J. Biol. Chem.* **277**, 5490-5497
46. Hoffmann, D., Gutekunst, K., Klissenbauer, M., Schulz-Friedrich, R., and Appel, J. (2006) Mutagenesis of hydrogenase accessory genes of *Synechocystis* sp. PCC 6803. Additional homologues of *hypA* and *hypB* are not active in hydrogenase maturation. *FEBS J.* **273**, 4516-4527
47. Funk, C., and Vermaas, W. (1999) A cyanobacterial gene family coding for single-helix proteins resembling part of the light-harvesting proteins from higher plants. *Biochemistry* **38**, 9397-9404
48. Jensen, P. E., Gibson, L. C., Henningsen, K. W., and Hunter, C. N. (1996) Expression of the *chlI*, *chlD*, and *chlH* genes from the Cyanobacterium *Synechocystis* PCC6803 in *Escherichia coli* and demonstration that the three cognate proteins are required for magnesium-protoporphyrin chelatase activity. *J. Biol. Chem.* **271**, 16662-16667
49. Leech, H. K., Raux, E., McLean, K. J., Munro, A. W., Robinson, N. J., Borrelly, G. P., Malten, M., Jahn, D., Rigby, S. E., Heathcote, P., and Warren, M. J. (2003) Characterization of the cobaltochelatase CbiXL: evidence for a 4Fe-4S center housed within an MXCXXC motif. *J. Biol. Chem.* **278**, 41900-41907
50. Stengel, A., Gugel, I. L., Hilger, D., Rengstl, B., Jung, H., and Nickelsen, J. (2012) Initial steps of photosystem II de novo assembly and preloading with manganese take place in biogenesis centers in *Synechocystis*. *Plant Cell* **24**, 660-675
51. Portnoy, M. E., Schmidt, P. J., Rogers, R. S., and Culotta, V. C. (2001) Metal transporters that contribute copper to metallochaperones in *Saccharomyces cerevisiae*. *Mol. Genet. Genomics* **265**, 873-882
52. Pope, C. R., De Feo, C. J., and Unger, V. M. (2013) Cellular distribution of copper to superoxide dismutase involves scaffolding by membranes. *Proc. Natl. Acad. Sci. U.S.A.* **110**, 20491-20496
53. Xiao, Z., and Wedd, A. G. (2002) A C-terminal domain of the membrane copper pump Ctr1 exchanges copper(I) with the copper chaperone Atx1. *Chem. Commun.* **21**, 588-589
54. Rowe, J. L., Starnes, G. L., and Chivers, P. T. (2005) Complex transcriptional control links NikABCDE-dependent nickel transport with hydrogenase expression in *Escherichia coli*. *J. Bacteriol.* **187**, 6317-6323
55. Chivers, P. T., Benanti, E. L., Heil-Chapdelaine, V., Iwig, J. S., and Rowe, J. L. (2012) Identification of Ni-(L-His)₂ as a substrate for NikABCDE-dependent nickel uptake in *Escherichia coli*. *Metallomics* **4**, 1043-1050
56. Chen, W., Dailey, H. A., and Paw, B. H. (2010) Ferrochelatase forms an oligomeric complex with mitoferrin-1 and Abcb10 for erythroid heme biosynthesis. *Blood* **116**, 628-630
57. Macomber, L., and Imlay, J. A. (2009) The iron-sulfur clusters of dehydratases are primary intracellular targets of copper toxicity. *Proc. Natl. Acad. Sci. U.S.A.* **106**, 8344-8349

58. Chillappagari, S., Seubert, A., Trip, H., Kuipers, O. P., Marahiel, M. A., and Miethke, M. (2010) Copper stress affects iron homeostasis by destabilizing iron-sulfur cluster formation in *Bacillus subtilis*. *J. Bacteriol.* **192**, 2512-2524
59. Ranquet, C., Ollagnier-de-Choudens, S., Loiseau, L., Barras, F., and Fontecave, M. (2007) Cobalt stress in *Escherichia coli*. The effect on the iron-sulfur proteins. *J. Biol. Chem.* **282**, 30442-30451
60. Thorgersen, M. P., and Downs, D. M. (2007) Cobalt targets multiple metabolic processes in *Salmonella enterica*. *J. Bacteriol.* **189**, 7774-7781
61. Tottey, S., Patterson, C. J., Banci, L., Bertini, I., Felli, I. C., Pavelkova, A., Dainty, S. J., Pernil, R., Waldron, K. J., Foster, A. W., and Robinson, N. J. (2012) Cyanobacterial metallochaperone inhibits deleterious side reactions of copper. *Proc. Natl. Acad. Sci. U.S.A.* **109**, 95-100
62. Frausto da Silva, J. J. R., and Williams, R. J. P. (1991) *The biological chemistry of the elements: the inorganic chemistry of life*, Oxford University Press, Oxford, New York.
63. Grubbs, R. D. (2002) Intracellular magnesium and magnesium buffering. *BioMetals* **15**, 251-259
64. Anbar, A. D. (2008) Oceans. Elements and evolution. *Science* **322**, 1481-1483
65. Hider, R. C., and Kong, X. L. (2011) Glutathione: a key component of the cytoplasmic labile iron pool. *BioMetals* **24**, 1179-1187
66. Williams, R. J. (1982) Free manganese (II) and iron (II) cations can act as intracellular cell controls. *FEBS Lett.* **140**, 3-10
67. McNaughton, R. L., Reddi, A. R., Clement, M. H., Sharma, A., Barnese, K., Rosenfeld, L., Gralla, E. B., Valentine, J. S., Culotta, V. C., and Hoffman, B. M. (2010) Probing *in vivo* Mn²⁺ speciation and oxidative stress resistance in yeast cells with electron-nuclear double resonance spectroscopy. *Proc. Natl. Acad. Sci. U.S.A.* **107**, 15335-15339
68. Maret, W. (2004) Zinc and sulfur: a critical biological partnership. *Biochemistry* **43**, 3301-3309
69. Krezel, A., and Maret, W. (2006) Zinc-buffering capacity of a eukaryotic cell at physiological pZn. *J. Biol. Inorg. Chem.* **11**, 1049-1062
70. Bozym, R. A., Thompson, R. B., Stoddard, A. K., and Fierke, C. A. (2006) Measuring picomolar intracellular exchangeable zinc in PC-12 cells using a ratiometric fluorescence biosensor. *ACS Chem. Biol.* **1**, 103-111
71. Vinkenborg, J. L., Nicolson, T. J., Bellomo, E. A., Koay, M. S., Rutter, G. A., and Merckx, M. (2009) Genetically encoded FRET sensors to monitor intracellular Zn²⁺ homeostasis. *Nat. Methods* **6**, 737-740
72. Wang, D., Hurst, T. K., Thompson, R. B., and Fierke, C. A. (2011) Genetically encoded ratiometric biosensors to measure intracellular exchangeable zinc in *Escherichia coli*. *J. Biomed. Opt.* **16**, 087011
73. Huang, C. P., Fofana, M., Chan, J., Chang, C. J., and Howell, S. B. (2014) Copper transporter 2 regulates intracellular copper and sensitivity to cisplatin. *Metallomics* **6**, 654-661
74. Dodani, S. C., Domaille, D. W., Nam, C. I., Miller, E. W., Finney, L. A., Vogt, S., and Chang, C. J. (2011) Calcium-dependent copper redistributions in neuronal cells revealed by a fluorescent copper sensor and X-ray fluorescence microscopy. *Proc. Natl. Acad. Sci. U.S.A.* **108**, 5980-5985
75. Rae, T. D., Schmidt, P. J., Pufahl, R. A., Culotta, V. C., and O'Halloran, T. V. (1999) Undetectable intracellular free copper: the requirement of a copper chaperone for superoxide dismutase. *Science* **284**, 805-808
76. Furukawa, Y., Torres, A. S., and O'Halloran, T. V. (2004) Oxygen-induced maturation of SOD1: a key role for disulfide formation by the copper chaperone CCS. *EMBO J.* **23**, 2872-2881
77. Xiao, Z., and Wedd, A. G. (2010) The challenges of determining metal-protein affinities. *Nat. Prod. Rep.* **27**, 768-789
78. Reyes-Caballero, H., Campanello, G. C., and Giedroc, D. P. (2011) Metalloregulatory proteins: metal selectivity and allosteric switching. *Biophys. Chem.* **156**, 103-114

79. Helmann, J. D. (2014) This set. *J. Biol. Chem*
80. Rutherford, J. C., and Bird, A. J. (2004) Metal-responsive transcription factors that regulate iron, zinc, and copper homeostasis in eukaryotic cells. *Eukaryot. Cell* **3**, 1-13
81. Li, L., Bagley, D., Ward, D. M., and Kaplan, J. (2008) Yap5 is an iron-responsive transcriptional activator that regulates vacuolar iron storage in yeast. *Mol. Cell. Biol.* **28**, 1326-1337
82. Waldron, K. J., and Robinson, N. J. (2009) How do bacterial cells ensure that metalloproteins get the correct metal? *Nat. Rev. Microbiol.* **7**, 25-35
83. Foster, A. W., Patterson, C. J., Pernil, R., Hess, C. R., and Robinson, N. J. (2012) Cytosolic Ni(II) sensor in cyanobacterium: nickel detection follows nickel affinity across four families of metal sensors. *J. Biol. Chem.* **287**, 12142-12151
84. Patterson, C. J., Pernil, R., Dainty, S. J., Chakrabarti, B., Henry, C. E., Money, V. A., Foster, A. W., and Robinson, N. J. (2013) Co(II)-detection does not follow Kco(II) gradient: channelling in Co(II)-sensing. *Metallomics* **5**, 352-362
85. Foster, A. W., Pernil, R., Patterson, C. J., and Robinson, N. J. (2014) Metal specificity of cyanobacterial nickel-responsive repressor InrS: cells maintain zinc and copper below the detection threshold for InrS. *Mol. Microbiol.* **92**, 797-812
86. Rutherford, J. C., Cavet, J. S., and Robinson, N. J. (1999) Cobalt-dependent transcriptional switching by a dual-effector MerR-like protein regulates a cobalt-exporting variant CPx-type ATPase. *J. Biol. Chem.* **274**, 25827-25832
87. Thelwell, C., Robinson, N. J., and Turner-Cavet, J. S. (1998) An SmtB-like repressor from *Synechocystis* PCC 6803 regulates a zinc exporter. *Proc. Natl. Acad. Sci. U.S.A.* **95**, 10728-10733
88. Outten, C. E., and O'Halloran, T. V. (2001) Femtomolar sensitivity of metalloregulatory proteins controlling zinc homeostasis. *Science* **292**, 2488-2492
89. Changela, A., Chen, K., Xue, Y., Holschen, J., Outten, C. E., O'Halloran, T. V., and Mondragon, A. (2003) Molecular basis of metal-ion selectivity and zeptomolar sensitivity by CueR. *Science* **301**, 1383-1387
90. Wang, D., Hosteen, O., and Fierke, C. A. (2012) ZntR-mediated transcription of *zntA* responds to nanomolar intracellular free zinc. *J. Inorg. Biochem.* **111**, 173-181
91. Alatosava, T., Jutte, H., Kuhn, A., and Kellenberger, E. (1985) Manipulation of intracellular magnesium content in polymyxin B nonapeptide-sensitized *Escherichia coli* by ionophore A23187. *J. Bacteriol.* **162**, 413-419
92. Mills, S. A., and Marletta, M. A. (2005) Metal binding characteristics and role of iron oxidation in the ferric uptake regulator from *Escherichia coli*. *Biochemistry* **44**, 13553-13559
93. Iwig, J. S., Leitch, S., Herbst, R. W., Maroney, M. J., and Chivers, P. T. (2008) Ni(II) and Co(II) sensing by *Escherichia coli* RcnR. *J. Am. Chem. Soc.* **130**, 7592-7606
94. Chivers, P. T., and Sauer, R. T. (2002) NikR repressor: high-affinity nickel binding to the C-terminal domain regulates binding to operator DNA. *Chem. Biol.* **9**, 1141-1148
95. Dann, C. E., 3rd, Wakeman, C. A., Sieling, C. L., Baker, S. C., Irnov, I., and Winkler, W. C. (2007) Structure and mechanism of a metal-sensing regulatory RNA. *Cell* **130**, 878-892
96. Ma, Z., Faulkner, M. J., and Helmann, J. D. (2012) Origins of specificity and cross-talk in metal ion sensing by *Bacillus subtilis* Fur. *Mol. Microbiol.* **86**, 1144-1155
97. Ma, Z., Cowart, D. M., Scott, R. A., and Giedroc, D. P. (2009) Molecular insights into the metal selectivity of the copper(I)-sensing repressor CsoR from *Bacillus subtilis*. *Biochemistry* **48**, 3325-3334
98. Ma, Z., Gabriel, S. E., and Helmann, J. D. (2011) Sequential binding and sensing of Zn(II) by *Bacillus subtilis* Zur. *Nucleic Acids Res.* **39**, 9130-9138
99. Grosseohme, N., Kehl-Fie, T. E., Ma, Z., Adams, K. W., Cowart, D. M., Scott, R. A., Skaar, E. P., and Giedroc, D. P. (2011) Control of copper resistance and inorganic sulfur metabolism by paralogous regulators in *Staphylococcus aureus*. *J. Biol. Chem.* **286**, 13522-13531
100. Pennella, M. A., Arunkumar, A. I., and Giedroc, D. P. (2006) Individual metal ligands play distinct functional roles in the zinc sensor *Staphylococcus aureus* CzrA. *J. Mol. Biol.* **356**, 1124-1136

Table and figure legends

Table 1. Types of metal sites and metal delivery pathways in Metal-MACiE.

Figure 1. Metallation is governed by metal availability for MncA and CucA. **a**, Mn(II)-MncA global fold. **b**, Cu(II)-CucA global fold. Both proteins adopt a cupin architecture, with MncA composed of two cupin domains. **c**, MncA N-terminal Mn(II) binding site. **d**, CucA Cu(II) binding site. Both proteins coordinate their metals with identical ligand sets, with a water molecule in the open coordination position (this position is occupied by acetate in the C-terminal Mn(II) binding site of MncA). MncA and CucA both prefer to bind copper rather than manganese *in vitro*, but MncA folds and traps manganese in the metal-regulated environment of the cytoplasm. PDB: 2VQA and 2XL7.

Figure 2. Correlation between buffered set points and metal-sensor affinities. Graphical representation of estimated intracellular buffered metal concentrations (grey bars) for magnesium, manganese, iron, cobalt, nickel, copper and zinc (62,65,66,72,73,90,91) and correlation with K_{Metal} of cytosolic metal-sensors for their cognate metal, including Fur (92), RcnR (93), NikR (94), CueR (89), Zur (88), and ZntR (88), from *E. coli* (red circles), the M-box riboswitch (95), MntR (96), Fur (96), CsoR (97), and Zur (98), from *B. subtilis* (blue triangles), CoaR (84), InrS (83), Zur (85), and ZiaR (85) from *Synechocystis* PCC 6803 (green diamonds), and CsoR (99), and CzrA (100), from *Staphylococcus aureus* (purple squares). It is hypothesised that K_{Metal} of metal-sensors maintains the set points for buffered metal concentrations as an inverse function of the Irving-Williams series.

Figure 3. Relative -affinity, -access and -allostery in a complement of metal-sensors influences the metals detected *in vivo*. **a**, Calculated fractional occupancy of InrS, ZiaR and CoaR with Ni(II), Zn(II) and Co(II) as the concentration of these elements changes: $\theta = [\text{Metal}]_{\text{buffered}} / (K_{\text{Metal}} + [\text{Metal}]_{\text{buffered}})$ using published K_{Metal} (83-85). **b**, Fractional occupancy of specific DNA (top) with apo- (dashed) and zinc-InrS (solid) and (bottom), apo- (dashed) and zinc-ZiaR (solid), as a function of protein concentration.

$$\Delta G_C = -RT \ln(K_{\text{DNA2}}/K_{\text{DNA1}}).$$

The simulated curves were generated using published K_{DNA} values (85), $[\text{DNA}] = 10 \text{ nM}$. The selective detection of nickel correlates with relative nickel affinity, of zinc with relative ΔG_C for zinc, but a major kinetic contribution (channelling) is invoked for cobalt.

Figure 4. Associative ligand-exchange with a polydisperse buffer. **i**, The transfer of zinc from InrS to ZiaR via a dissociative release of zinc from InrS to a hydrated state. **ii**, The transfer of zinc from InrS to ZiaR by (potentially swift) associative ligand-exchange via a partly (x) zinc-saturated number of ligands (y) of a polydisperse buffer (L).

Table 1.

Metal	Site Type	Example enzyme from Metal-MACiE ¹	Delivery Pathway/Chaperone	% of Metal-MACiE total ^{2, 3}
Magnesium	Mononuclear	Adenylate cyclase (M0058)	None known	38
	Trinuclear (Mg)	Trichodiene synthase (M0262)	None known	3
Manganese	Mononuclear	Xylose isomerase (M0308)	None known	8
	Trinuclear (Mn or Zn)	Deoxyribonuclease IV (M0011)	None known	<1
Iron	Mononuclear	Catechol-2,3-dioxygenase (M0034)	None known	3
	Dinuclear (FeFe)	Ferredoxin hydrogenase (M0127)	HydE/G provide iron as[FeS], production of which is dependent on CyaY	<1
	Dinuclear (NiFe)	Cytochrome-c3 hydrogenase (M0126)	Assembly of cyano-, carbonyl-coordinated iron occurs on HypD. Source of iron is unknown	<1
	Dinuclear (ZnFe)	Purple acid phosphatase (M0043)	None known	<1
	Heme	Ubiquinol-cytochrome-c reductase (M0208)	Iron chelatase	7
	Iron-sulphur cluster	Aldehyde oxidase (M0105)	CyaY	14
Cobalt	Mononuclear	Thiocyanate hydrolase (M0284)	None known	2
	Cobalmin	Methionine synthase (M0268)	CbiX	2
Nickel	Dinuclear (NiFe)	Cytochrome-c3 hydrogenase (M0126)	HypA/ HypB/ SlyD	<1
	Dinuclear (NiNi)	Urease (M0087)	UreE/ UreG	<1
	Factor-430	Coenzyme-B sulfoethylthiotransferase (M0156)	None known	<1
Copper	Mononuclear	Copper-zinc SOD (M0138)	CCS (and others)	2 ⁴ 1 ⁵
	Dinuclear (CuCu)	Tyrosinase (M0125)	Atx1 (and others)	1
	Dinuclear (CuMo)	Carbon-monoxide dehydrogenase (M0107)	None known	<1
Zinc	Mononuclear	Alcohol dehydrogenase (M0256)	None known	11
	Dinuclear (ZnZn)	Beta lactamase (M0015)	None known	2
	Dinuclear (ZnFe)	Purple acid phosphatase (M0043)	None known	<1
	Trinuclear (Zn)	Phospholipase C (M0027)	None known	1
Molybdenum	Molybdopterin	Xanthine dehydrogenase (M0139)	MoeA	2
	FeMo-cofactor	Nitrogenase (M0212)	CyaY, NifH	<1

	Dinuclear (CuMo)	Carbon-monoxide dehydrogenase (M0107)	None known	<1
--	---------------------	--	------------	----

¹ Metal-MACiE identifier shown in parenthesis

² Total excludes calcium enzymes represented in Metal-MACiE

³ Hetero-dinuclear sites count as one site for each metal ion, homo di- and tri-nuclear sites count as one site

⁴ Known delivery pathways

⁵ Unknown delivery pathways

Figure 1.

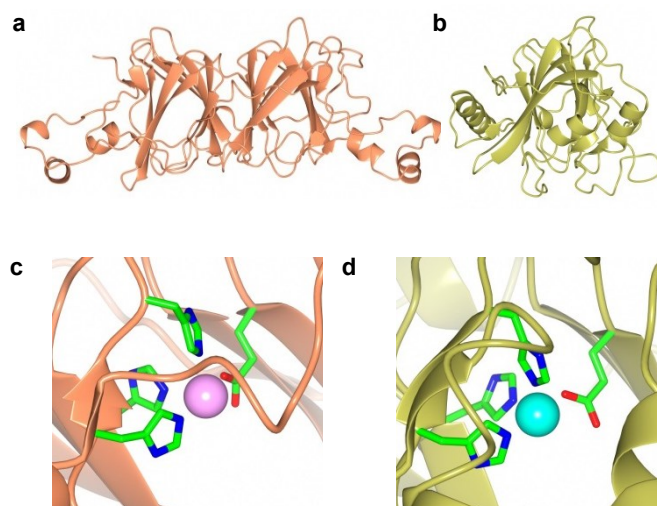


Figure 2.

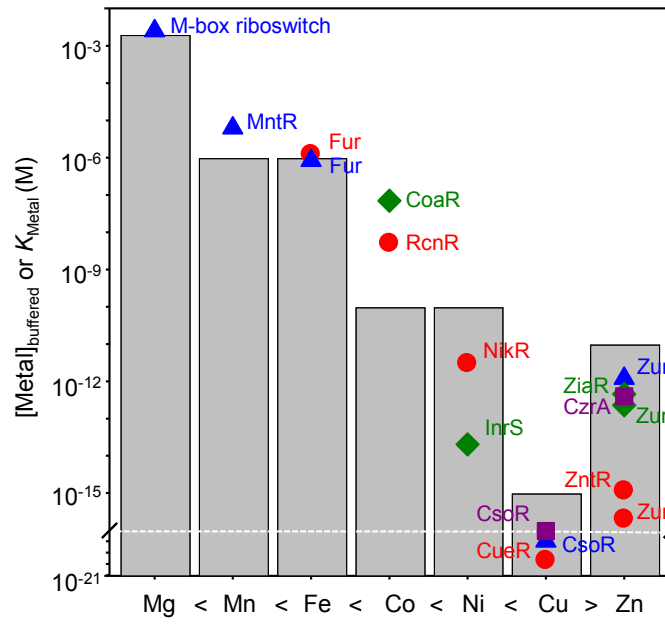


Figure 3.

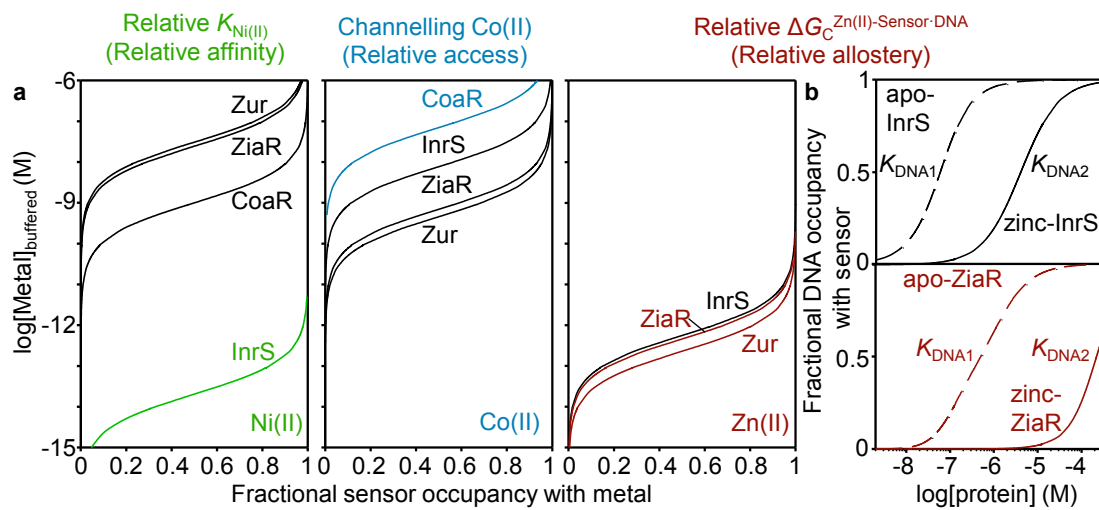


Figure 4.

- i. $\text{Zn.InrS} + \text{ZiaR} \leftrightarrow \text{Zn} + \text{InrS} + \text{ZiaR} \leftrightarrow \text{InrS} + \text{Zn.ZiaR}$
- ii. $\text{Zn.InrS} + \text{ZiaR} + \text{Zn}_x\text{L}_y \leftrightarrow \text{InrS} + \text{ZiaR} + \text{Zn}_{(x+1)}\text{L}_y \leftrightarrow \text{InrS} + \text{Zn.ZiaR} + \text{Zn}_x\text{L}_y$